Nondegenerate Parametric Resonance in Large Ensembles of Coupled Micromechanical Cantilevers with Varying Natural Frequencies

Christopher B. Wallin[1,2], Roberto De Alba[1,2], Nir Dick[3], Daron Westly[1], Glenn Holland[1], Scott Grutzik[4], Alan T. Zehnder[5], Richard H. Rand[5,6], Vladimir Aksyuk[1], Slava Krylov[3], and B. Robert Ilic[1]

[1]Physical Measurement Laboratory, National Institute of Standards and Technology, Gaithersburg, MD 20899
[2]Maryland Nanocenter, University of Maryland, College Park, MD 20742
[3]School of Mechanical Engineering, Tel Aviv University, Ramat Aviv 69978, Tel Aviv, Israel
[4]Component Science and Mechanics, Sandia National Laboratories, Albuquerque, NM 87185
[5]Department of Mechanical and Aerospace Engineering, Cornell University, Ithaca, NY 14853
[6]Department of Mathematics, Cornell University, Ithaca, NY 14853
robert.ilic@nist.gov

With the emergence of micro and nanoelectromechanical systems (M/NEMS) in recent decades, M/NEMS resonator arrays have been increasingly employed in the practical study of the complex, collective behavior of coupled oscillator systems. These M/NEMS resonator arrays have been shown to exhibit a host of nontrivial dynamics due predominantly to their nonlinear nature including intrinsically localized modes, abrupt pattern switching, multistability, hysteresis, and synchronization. With our work, we investigated both theoretically and experimentally the collective dynamics and nondegenerate parametric resonance (NPR) of coplanar, interdigitated arrays of microcantilevers distinguished by their cantilevers having linearly expanding lengths and thus varying natural frequencies.

Within a certain excitation frequency range and for sufficiently large drive amplitudes, the arrays of single-crystal silicon microcantilevers began oscillating via NPR. The distinctive device topology as shown in Fig. 1 produced spatially confined mode structures with tunable mode-to-mode coupling between opposing arrays that was generated through the asymmetries in the electrostatic fringing fields between neighboring cantilevers. Experimental verification of first-order NPR actuation within our system was determined using a two-dimensional cross-correlation normal mode matching algorithm as highlighted in Fig. 2. Our experimental results are supported by a reduced order model based on the Galerkin decomposition which generated the leading features of our data including the NPR band as illustrated in Fig. 3.

Exploiting NPR in future engineered M/NEMS could facilitate device operation at a multitude of frequencies, possibly enabling bandwidth expansion through frequency conversion and greater tunability of M/NEMS devices for applications such as resonance-based sensing. The high sensitivity of these coupled arrays to environmental perturbations will likely open new and interesting sensing scenarios based on NPR-actuated collective pattern recognition rather than on the frequency monitoring of individual elements. Lastly, the potential for tailoring the coupled response of suspended mechanical structures using NPR presents new possibilities in mass, force, and energy sensing applications, energy harvesting devices, and optomechanical systems.

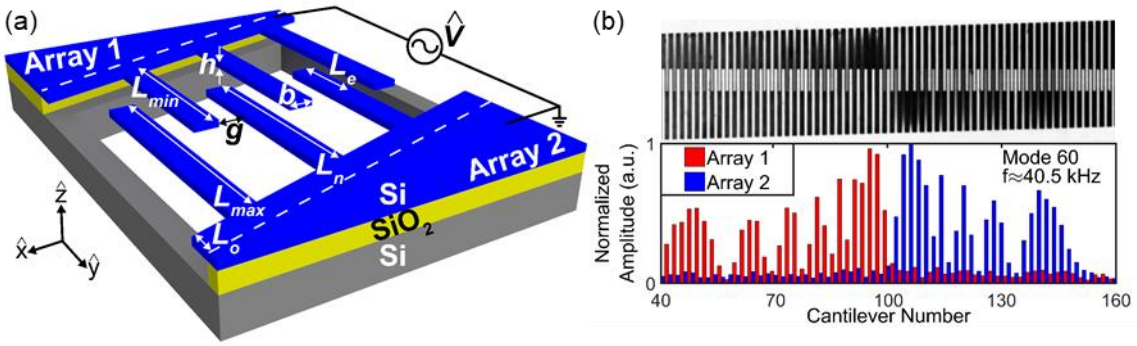

FIG. 1. (a) Schematic of the interdigitated, variable length microcantilever arrays. The actual device has 200 cantilevers. (b) An optical micrograph (top) of the center of the device being actuated at a drive frequency of $f_D \approx 40.5$ kHz. The spatially averaged grayscale pixel values (bottom) are obtained from the end of each cantilever providing a qualitative estimate of the out-of-plane vibrational amplitude for every cantilever on the device.

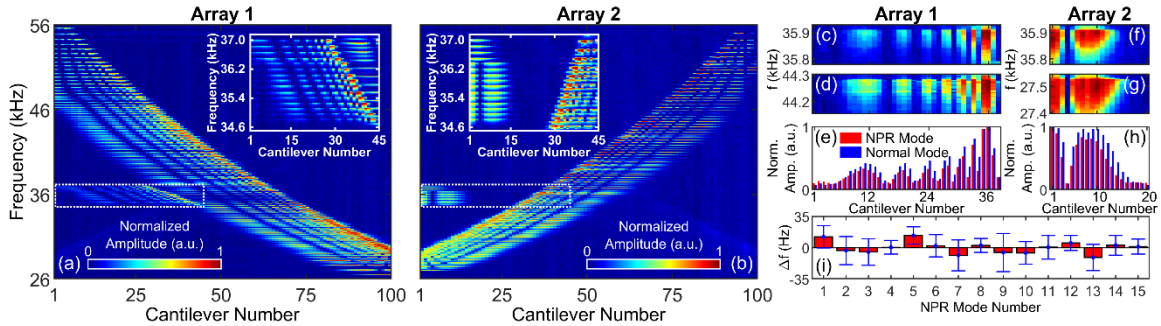

FIG. 2. The frequency response and NPR excitation of (a) array 1 and (b) array 2 driven at $\hat{V}_{ac} \approx 40$ V. The 15 observed NPR modes are featured within the dotted rectangles and are replotted in their respective insets. As an example of the results obtained from the normal mode matching algorithm, we have (c) NPR mode 8 and (d) the maximally correlated normal mode, both from array 1, showing almost indistinguishable mode structures. (e) Modal shapes produced by summing over frequency space using array 1's NPR mode 8 and its maximally correlated normal mode, further indicating nearly identical features. (f) NPR mode 8, (g) the maximally correlated normal mode, and (h) the modal shapes, all from array 2, illustrating strong similarity between the two modes. (i) The frequency deviation, Δf, from the NPR frequency condition conclusively demonstrates that the 15 modes outlined above are excited via the NPR mechanism.

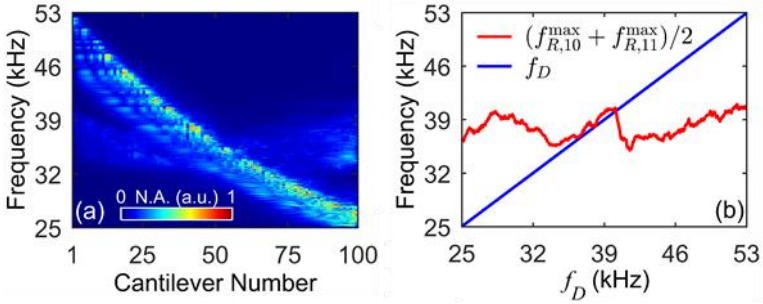

FIG. 3. (a) The numerically calculated down-chirped frequency response of array 1 with $\hat{V}_{ac} = 100$ V showing a NPR band from ≈ 33 to ≈ 40 kHz. (b) Summation of the numerically calculated peak frequency response for beams 10 and 11. Within the NPR region, the summed peak frequency response of beam 10, $f_{R,10}^{\max}$, and beam 11, $f_{R,11}^{\max}$, follow the NPR relation $f_D \approx \left(f_{R,10}^{\max} + f_{R,11}^{\max}\right)/2$, where f_D is the drive frequency.